Noncentrosymmetric Lamellar Phase in ABCD Tetrablock Copolymers

Karim M. Jaffer,[†] Robert A. Wickham,[‡] and An-Chang Shi[†,*]

Department of Physics and Astronomy, McMaster University, Hamilton, ON L8S 4M1, Canada, and Department of Physics, St. Francis Xavier University, Antigonish, NS B2G 2W5, Canada

Received February 1, 2004; Revised Manuscript Received June 29, 2004

ABSTRACT: The phase behavior of ABCD tetrablock copolymer melts is studied using self-consistent mean-field theory. In particular, the noncentrosymmetric (NCS) lamellar phase (with sequence ...ABCDABCD...) and the centrosymmetric (CS) lamellar phase (...ABCDDCBA...) are examined in two cases. First, an enthalpically stabilized NCS lamellar phase is investigated by varying the interaction between the A and D blocks from repulsive to attractive while keeping all block lengths equal. In the second case, an entropically stabilized NCS lamellar phase is investigated by changing the lengths of the two end blocks, which are taken to be chemically identical (ABCA tetrablock melt). In both cases, the NCS phase is found in regions of the phase diagram, and direct disorder to NCS transitions are possible. In addition, two partially mixed centrosymmetric (MCS) lamellar phases are observed between the disordered and fully ordered (NCS and CS) phases. This study extends our previous work on triblock−diblock blends which revealed an entropically stabilized noncentrosymmetric lamellar phase.

1. Introduction

Noncentrosymmetric (NCS) materials, which lack a center of symmetry in the absence of an external polarizing field, are rare in nature but have many potential applications, from piezoelectric materials[2] to optical second harmonic generations.[2,3] This technological potential has resulted in great interest in NCS materials.[1−6] Recent experiments have demonstrated the possibility of a self-assembled NCS phase in block copolymer blends.[6] Block copolymers consist of two or more covalently bonded subchains, or blocks, of chemically distinct monomers.[7,8] The competition between the constraint that the blocks are attached in a specific architecture and the repulsion between the unlike blocks leads to the formation of various ordered structures with periods of the order of tens of nanometers.[2,3] Furthermore, block copolymers can be tailor-made to attain the properties of a specific application. For example, the length of segments and overall degree of polymerization can be tuned to produce a specific wavelength for second harmonic generation.[3] NCS structures created using block copolymers have been shown to have longer periods than those created previously using small molecules.[2,3] The dielectric properties of the blocks can also be tailored. In addition, since block copolymers self-assemble into ordered periodic structures, no microfabrication techniques are necessary to produce the desired structure. The major obstacle to their use in practical applications is the absence of long-range order in the self-assembled structures. Achieving long range order in block copolymers presents a major challenge, and active research is being carried out.[7,8]

Pure diblock copolymer melts have a well-known phase diagram,[9] exhibiting lamellar, hexagonally packed cylindrical, body-centered cubic spherical and gyroid phases. All of these structures are centrosymmetric. Pure triblock copolymer melts can form a variety of phases (see refs 10 and 11), but almost all of these phases also have a center of symmetry.[12] The experiments in ref 6 on blends of ABC triblock and ac diblock copolymers demonstrated the formation of NCS structures not previously accessible using pure triblock melts.[11] Here A, B, and C refer to the chemical species of each block on the triblock and a and c those on the diblock. Only lamellar structures were reported in these experiments. The NCS lamellar phase in ABC and ac blends has been studied using self-consistent mean-field theory (SCMFT),[1] as well as strong segregation theory.[13−15] With the complexity of the phase diagrams for blends, as well as for multiblock copolymers, theoretical phase diagrams will be useful to experimental searches for the NCS structure. Reference 1 indicates the existence of a NCS lamellar phase in the blend phase space, but for the majority of the phase space there is two-phase coexistence between NCS and centrosymmetric phases. This behavior is consistent with the experimental results.[6] When producing a NCS phase, it is desirable to have a direct transition from the disordered to NCS phase in order to avoid the possibility that the system becomes kinetically trapped in an intermediate phase. In the blend system, such direct transitions do not occur. To address both of these issues, the existence of NCS lamellar phases in linear ABCD tetrablock copolymer melts is investigated using SCMFT. The presence of a fourth block creates an added complexity to the phase diagram.[16,17] It also provides the opportunity for the formation of a pure NCS phase, as demonstrated by this work and in recent experiments.[18,19]

Figure 1 depicts the possible lamellar structures formed by ABCD tetrablock copolymer melts. The first two structures are the fully ordered, centrosymmetric (CS) and noncentrosymmetric (NCS), lamellar phases. The three additional lamellar structures are partially ordered phases which are examined in this study. Lamellar CS and NCS phases in ABCD and ABCA tetrablock melts have been recently observed in experiments by Takano et al.[18,19] From an enthalpic perspective, an attractive interaction between the outer A and D blocks[20] should favor the sequence (...ABCDABCD...) leading to a NCS lamellar phase. The attractive A−D

* Corresponding author. E-mail: shi@mcmaster.ca.
[†] McMaster University.
[‡] St. Francis Xavier University.

10.1021/ma049784h CCC: $27.50
Published on Web 08/13/2004

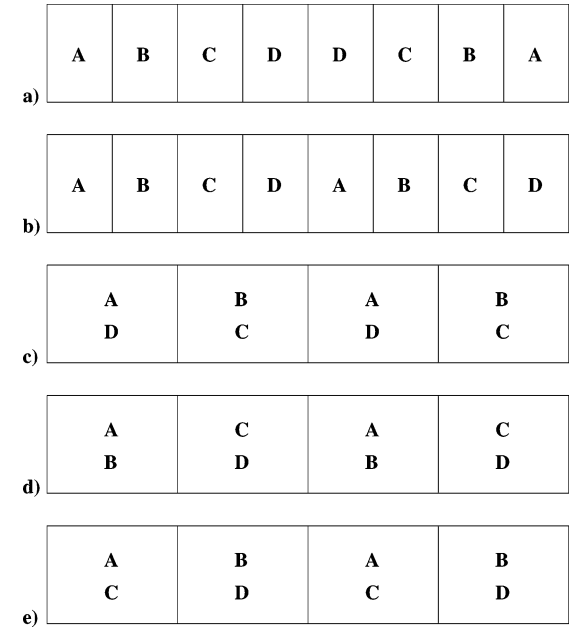

Figure 1. Possible lamellar structures for ABCD tetrablock copolymer melts. The fully ordered structures are (a) centrosymmetric (CS) and (b) noncentrosymmetric (NCS). There are three possible partially ordered (mixed) lamellar structures, (c) mixed centrosymmetric BC (MCS BC), (d) mixed centrosymmetric AB (MCS AB) and (e) mixed centrosymmetric AC (MCS AC).

interaction is represented by a negative Flory−Huggins parameter χ_{AD} in the theory. Previous theoretical studies[1,13,15] demonstrated that it is also possible to stabilize a NCS lamellar phase through an entropic mechanism. In the current study, the entropic effects are investigated by varying the compositions of the outer blocks for the case of ABCA tetrablock copolymer melts (A and D blocks being chemically identical). For simplicity, the investigations are limited to lamellar structures. We compare our results to recent experiments.[18,19]

2. Self-Consistent Mean-Field Theory

We consider an incompressible ABCD tetrablock copolymer melt in a volume V. The degree of polymerization of the tetrablock is N, with each block having a degree of polymerization $f_\alpha N$ with α = A, B, C, or D. The composition variables, f_α, satisfy $f_A + f_B + f_C + f_D = 1$. Distances are scaled by the Gaussian radius of gyration for the tetrablock, $R_g = b(N/6)^{1/2}$. For simplicity, the monomer statistical Kuhn length b and the bulk monomer density ρ_0 are assumed to be the same for all four chemical species. The chain arc length is scaled by the tetrablock degree of polymerization N.

Beginning with the many-chain Edwards Hamiltonian, the free-energy F of the melt can be derived in the mean-field approximation.[21] The suitably scaled free-energy density f at temperature T has the form

$$f \equiv \frac{NF}{\rho_0 V k_B T} = \frac{1}{V}\int d\mathbf{r}\left\{\frac{1}{2}\sum_{\alpha\neq\beta}\chi_{\alpha\beta}\phi_\alpha(\mathbf{r})\phi_\beta(\mathbf{r}) - \sum_{\alpha=A,B,C,D}\omega_\alpha(\mathbf{r})\phi_\alpha(\mathbf{r})\right\} - \ln Q[\omega] \quad (1)$$

where $\phi_\alpha(\mathbf{r})$ denotes the volume fraction of α monomers at position $\mathbf{r}$. The monomer−monomer interactions are modeled by the six Flory−Huggins parameters χ_{AB}, χ_{AC}, χ_{AD}, χ_{BC}, χ_{BD}, and χ_{CD}.

In eq 1, $Q[\omega]$ is the partition function of a single tetrablock copolymer interacting with the mean-fields $\omega_\alpha(\mathbf{r})$. This partition function may be written in terms of the propagators $Q_\alpha(\mathbf{r}, s|\mathbf{r}')$, which give the probability that the α monomer at arc length s is at position $\mathbf{r}$, given that the α monomer at arc length 0 is at $\mathbf{r}'$:

$$Q[\omega] = \frac{1}{V}\int d\mathbf{r}_1\cdots d\mathbf{r}_5 Q_A(\mathbf{r}_1, f_A|\mathbf{r}_2)Q_B(\mathbf{r}_2, f_B|\mathbf{r}_3)\times Q_C(\mathbf{r}_3, f_C|\mathbf{r}_4)Q_D(\mathbf{r}_4, f_D|\mathbf{r}_5) \quad (2)$$

The factors of $1/V$ are inserted above for convenience. The propagators satisfy the modified diffusion equation

$$\frac{\partial}{\partial s}Q_\alpha(\mathbf{r}, s|\mathbf{r}') = \nabla^2_{\mathbf{r}}Q_\alpha(\mathbf{r}, s|\mathbf{r}') - \omega_\alpha(\mathbf{r})Q_\alpha(\mathbf{r}, s|\mathbf{r}') \quad (3)$$

with the initial condition

$$Q_\alpha(\mathbf{r}, 0|\mathbf{r}') = \delta(\mathbf{r} - \mathbf{r}') \quad (4)$$

In the mean-field approximation, the fields ω_α are related to the monomer volume fractions ϕ_α through the following relations:

$$\omega_A(\mathbf{r}) = \chi_{AB}N\,\phi_B(\mathbf{r}) + \chi_{AC}N\,\phi_C(\mathbf{r}) + \chi_{AD}N\,\phi_D(\mathbf{r}) + \eta(\mathbf{r}) \quad (5)$$

$$\omega_B(\mathbf{r}) = \chi_{AB}N\,\phi_A(\mathbf{r}) + \chi_{BC}N\,\phi_C(\mathbf{r}) + \chi_{BD}N\,\phi_D(\mathbf{r}) + \eta(\mathbf{r}) \quad (6)$$

$$\omega_C(\mathbf{r}) = \chi_{AC}N\,\phi_A(\mathbf{r}) + \chi_{BC}N\,\phi_B(\mathbf{r}) + \chi_{CD}N\phi_D(\mathbf{r}) + \eta(\mathbf{r}) \quad (7)$$

$$\omega_D(\mathbf{r}) = \chi_{AD}N\,\phi_A(\mathbf{r}) + \chi_{BD}N\,\phi_B(\mathbf{r}) + \chi_{CD}N\,\phi_C(\mathbf{r}) + \eta(\mathbf{r}) \quad (8)$$

where the field $\eta(\mathbf{r})$ is to be adjusted to enforce the incompressibility condition:

$$\phi_A(\mathbf{r}) + \phi_B(\mathbf{r}) + \phi_C(\mathbf{r}) + \phi_D(\mathbf{r}) = 1 \quad (9)$$

The monomer volume fractions are, in turn, related to the functional derivative of ln $Q[\omega]$:

$$\phi_\alpha(\mathbf{r}) = -V\frac{\delta \ln Q[\omega]}{\delta\omega_\alpha(\mathbf{r})} \quad (10)$$

These functional derivatives are evaluated using eqs 2−4.

Equations 5−10 form a set of self-consistent equations between the ϕ_α and the ω_α. The *exact* mean-field solution for a given point in the phase space can be obtained from these equations using numerical methods. The method of solution involves selecting a set of basis functions appropriate to the periodic structure to be examined. The theory is then re-formulated in terms of expansion coefficients using these basis functions.[9] Using initial guesses for the period, D, and monomer profiles, ϕ_α, of the structure, the reciprocal space versions of eqs 5−10 are solved iteratively to obtain the mean-field profiles and free-energy density f corresponding to the chosen D. This procedure is repeated for different choices of D to yield a minimum free-energy density at the system's preferred period. The numerical procedure and the

reciprocal space formulation are discussed in more detail in refs 9, 22, and 23. For each possible structure, the above calculation must be performed to find the preferred period and minimal free-energy density for each point in phase space. These free-energy densities are compared and the structure with the lowest f at that point in phase space is the equilibrium structure.

A pure triblock copolymer melt can form many different periodic structures.[10,11] The number of structures formed by tetrablock copolymers is even larger, with a much larger parameter space. Our current investigation focuses on the study of lamellar phases. This reduces the problem to a one-dimensional structure, with cosines and sines as basis functions. The monomer volume fractions and the mean-fields for a lamellar modulation chosen to be along the z-axis are given by

$$\phi_\alpha(z) = \sum_{n=0}^{\infty} \phi_{\alpha,n}^{(c)} \cos\left(\frac{2\pi n}{D} z\right) + \sum_{n=1}^{\infty} \phi_{\alpha,n}^{(s)} \sin\left(\frac{2\pi n}{D} z\right) \quad (11)$$

$$\omega_\alpha(z) = \sum_{n=0}^{\infty} \omega_{\alpha,n}^{(c)} \cos\left(\frac{2\pi n}{D} z\right) + \sum_{n=1}^{\infty} \omega_{\alpha,n}^{(s)} \sin\left(\frac{2\pi n}{D} z\right) \quad (12)$$

where $\phi_{\alpha,n}^{(c)}$ and $\phi_{\alpha,n}^{(s)}$ are the respective Fourier amplitudes of the cosines and sines for the monomer volume fractions, and $\omega_{\alpha,n}^{(c)}$ and $\omega_{\alpha,n}^{(s)}$ for the mean-fields. These amplitudes are determined self-consistently from eqs 5−10. The noncentrosymmetric phase was obtained using both sines and cosines and an initial monomer profile that was NCS (...ABCDABCD...) to begin the iteration procedure. Centrosymmetric phases (...ABCDDCBA...) have only cosines as basis functions ($\phi_{\alpha,n}^{(s)} = \omega_{\alpha,n}^{(s)} = 0 \; \forall \; \alpha, n$). Additional lamellar structures will be discussed in the next section.

In the numerical computation the number of basis functions used in the expansions 11 and 12 is finite. Greater accuracy in the free energy density is achieved by increasing the number of basis functions, but at a computational cost in time and memory. The number of basis functions in the computation of the free-energy density, which is $O(1)$, is selected to achieve an accuracy of 10^{-6}. This level of accuracy is sufficient to resolve the free-energy differences between the various phases. For example, at $\chi N = 32$, convergence of the CS and MCS phases require 25 basis functions for this accuracy, while the NCS phase requires 50 (25 sines and 25 cosines). The number of basis functions needed increases as a function of χN and the complexity of the phases.

3. Results and Discussion

The parameter space for the tetrablock copolymer system is extremely large: χ_{AB}, χ_{AC}, χ_{AD}, χ_{BC}, χ_{BD}, χ_{CD}, N, f_A, f_B, and f_C can all be varied independently. Conducting a full search of the phase diagram for the system is beyond the scope of the present work. Instead, only lamellar structures (as depicted in Figure 1) are considered in the current paper. With judicious selections for the parameters, it should be possible, using previous studies[1,9,10] as guides, to restrict the study to the lamellar region of the phase diagram.

We examine two mechanisms for the formation of the NCS lamellar phase. The enthalpically stabilized NCS lamellar phase is investigated by changing the interaction parameter between the A and D blocks, χ_{AD} (see Figure 2), while keeping block compositions fixed. All the other $\chi_{\alpha\beta}$ are kept equal to each other, thus $\chi_{\alpha\beta} = \chi$ except χ_{AD}. While keeping all $\chi_{\alpha\beta}$ equal may not represent a physical block copolymer system, this choice allows us to focus on the effect of the interaction between the outer blocks. Extension of the calculations to block copolymers with different Flory−Huggins parameters is straightforward. Using the lamellar behavior of diblocks as a reference,[1,9] all four block compositions are set equal ($f_A = f_B = f_C = f_D = 0.25$). The equality of the tetrablock compositions prevents curved interfaces so that layered structures should prevail.

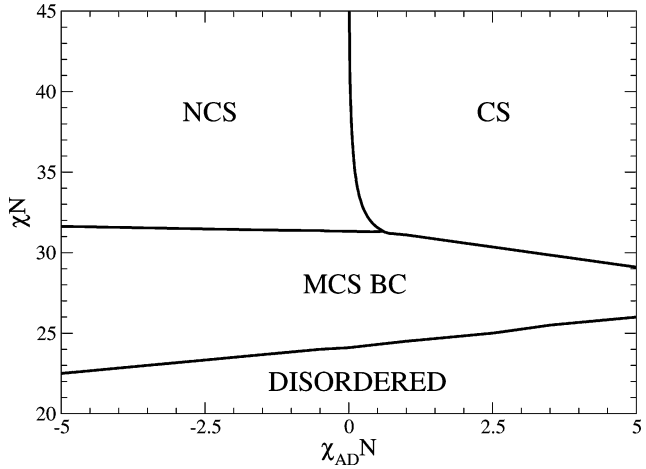

Figure 2. Mean-field phase diagram for ABCD tetrablock copolymer melts with $f_\alpha = 1/4$. The Flory−Huggins parameters are $\chi_{\alpha\beta} = \chi$ except χ_{AD}.

The entropically stabilized NCS lamellar phase is investigated by changing block compositions for a special class of tetrablocks (ABCA). The outer blocks are chemically identical, given by $\chi_{AD} = 0$, while the inner block enthalpic interactions are kept equal, $\chi_{AB} = \chi_{AC} = \chi_{BC} = \chi_{BD} = \chi_{CD} = \chi$. The inner B and C block compositions are kept equal ($f_B = f_C$) in the entropic study such that lamellar phases are favored.

3.1. Enthalpic Effects. The NCS lamellar phase (...ABCDABCD...) will have a lower free energy than the CS lamellar phase (...ABCDDCBA...) when the system has a preference for the A:D interfaces. An attractive interaction between the A and D blocks[20] should favor A:D interfaces. Previous studies[2−5] have argued that the chemical interactions required to achieve this attraction[20] are also necessary for electronic applications requiring ferroelectric, piezoelectric and pyroelectric behavior. To examine the effect of the A−D interaction, χ_{AD} is varied from slightly negative (A and D blocks attract each other) to slightly positive (repulsive interactions between the A and D blocks). Throughout this range, $|\chi_{AD}| < |\chi|$. SCMFT calculations for this system yield a phase diagram in the $\chi_{AD}N - \chi N$ plane as shown in Figure 2.

At low χN, the system is in a disordered state. The order−disorder transition boundary $(\chi N)_{ODT}$ follows approximately a straight line, changing from $(\chi N)_{ODT} \simeq 22.5$ at $\chi_{AD}N = -5$ to $(\chi N)_{ODT} \simeq 26$ at $\chi_{AD}N = 5$. The values of $(\chi N)_{ODT}$ are higher than that for diblock copolymers.[9] As we increase χN, the first ordered phase in this phase diagram is a mixed centrosymmetric (MCS BC) phase (see Figure 1c), where the two outer blocks are still mixed together, as are the two inner blocks (B and C). The monomer density profile for this phase is shown in Figure 3. In this region of the phase diagram, the block interactions are strong enough such that a fully disordered phase is not favored. On the other hand,

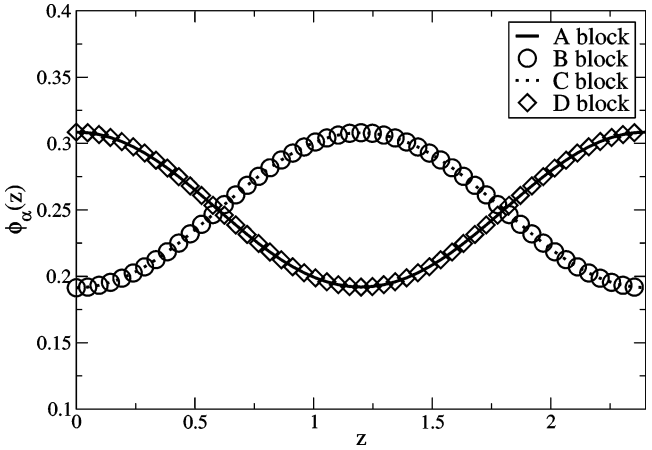

Figure 3. Monomer density profile of the mixed centrosymmetric BC lamellar phase (MCS BC) of the ABCD tetrablock copolymer melt with $f_\alpha = {}^1/_4$, $\chi N = 28$,$\chi_{AD}N = 0.3$.

χN is not large enough to separate the B and C blocks, leading to a mixed phase (MCS BC).

As χN is increased, the B and C blocks will separate. The transition to fully separated phases has very different behavior depending on whether χ_{AD} is negative or positive, with additional complexity near $\chi_{AD} = 0$. The NCS phase is observed in a large region of phase space where the A and D blocks are attracted to each other and all other $\chi N \geq 31.5$. The presence of the NCS phase is intuitively obvious since a negative χ_{AD} favors interfaces between the A and D blocks vs A:A and D:D interfaces. In the region where $\chi_{AD}N > 0$, the system does not prefer A:D interfaces, thus the CS phase becomes favored. The monomer density profile for the CS phase is shown in Figure 4a, and the NCS phase profile is shown in Figure 4b.

For the special case where $\chi_{AD}N = 0$, the system becomes an ABCA tetrablock copolymer melt, since the Kuhn length and bulk monomer densities are assumed equal for all chemical species. In this case there is no enthalpic gain for the NCS structure over the CS structure. Thus, it is a surprise that at $\chi N > 31.3$, the NCS structure has the lower free energy density. The NCS lamellar phase for ABCA copolymers will be studied in greater detail in the next section (on entropic effects). The occurrence of the NCS phase in the region $\chi_{AD}N > 0$, for a small range around $\chi N \simeq 31.5$, indicates that the entropic effects for ABCA tetrablock copolymers are strong enough to overcome a slight enthalpic penalty between the outer blocks for ABCD tetrablocks.

Turning back to the $\chi_{AD} < 0$ region, it is interesting to see if a direct disorder to NCS phase transition is possible. In Figure 2, the MCS BC phase is observed between the disordered and NCS phases. For a given value of $\chi_{AD}N$, increasing $\chi_{BC}N$ from the common χN should lead to the separation of the B and C blocks, thus destabilizing the MCS BC phase. This may yield a direct disorder to NCS phase transition. From Figure 2, there are three areas of the phase diagram which may exhibit different behavior when χ_{BC} is varied from χ. First, a cut in the region $\chi_{AD} < 0$ can be examined. Second, investigating the $\chi_{AD} = 0$ cut of the phase diagram (ABCA tetrablocks) may yield different behavior from the first case. Third, the lip region of the NCS phase can be investigated, where the interaction between A the D blocks is slightly repulsive. The mean-field results for these different cuts are shown in Figure 5.

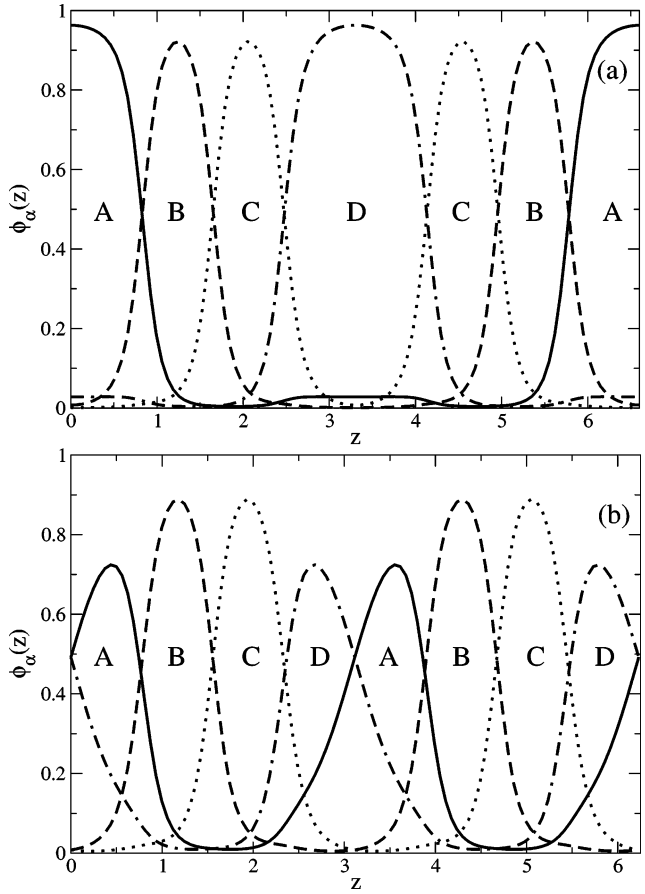

Figure 4. Monomer density profiles for the ABCD tetrablock copolymer melt with $f_\alpha = {}^1/_4$, $\chi_{AD}N = 0.3$ for (a) one period of the centrosymmetric (CS) lamellar phase at $\chi N = 35$, and (b) two periods of the noncentrosymmetric (NCS) lamellar phase at $\chi N = 32.3$. For both sets of profiles, the solid line represents $\phi_A(z)$, the dashed line $\phi_B(z)$, the dotted line $\phi_C(z)$, and the dash−dotted line $\phi_D(z)$, respectively.

The phase diagram for the first of these cuts is shown in Figure 5a for $\chi_{AD}N = -5.0$. As expected, the MCS BC region decreases in size as $\chi_{BC}N$ increases (left to right in Figure 5a). The increase in repulsion between the B and C blocks eventually overcomes both the enthalpic gain from mixing the A and D blocks and the entropic penalty from stretching to a fully ordered arrangement. This is reflected in the increasing value for $(\chi N)_{ODT}$ and the decreasing χN at the transition to the NCS phase as $\chi_{BC}N$ increases. Correspondingly, the NCS region becomes larger, resulting in a direct disorder to NCS phase transition in a small window in the phase diagram around $\chi_{BC}N \simeq 42$. Interestingly, a new mixed phase, MCS AB (see Figure 1d), exists at large values of χ_{BC} and small values of χN. The monomer density profile for the MCS AB phase is shown in Figure 6. As $\chi_{BC}N$ increases, it eventually becomes strong enough to demix the B and C blocks. When this occurs, the outer blocks are taken into these domains, mixing the A with B and C with D blocks. Examining the amplitudes of the monomer densities in Figure 6, there is still a substantial degree of mixing between the A and D blocks in the MCS AB phase. The MCS AB phase is much different than the MCS BC phase as is evident by comparing Figures 3 and 6.[24]

The second cut is taken for the special case of ABCA tetrablocks, $\chi_{AD} = 0$. The mean-field phase diagram for this case is nearly identical to the previous cut (Figure

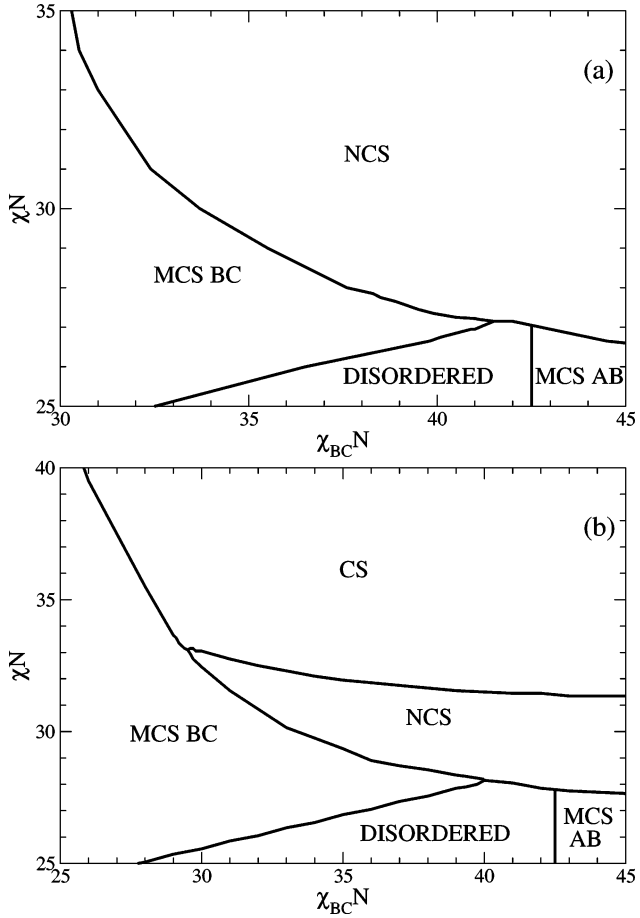

Figure 5. Mean-field phase diagram for the ABCD tetrablock copolymer melt with $f_\alpha = {}^1/_4$. The Flory−Huggins parameters are $\chi_{\alpha\beta} = \chi$ except χ_{BC} and χ_{AD}. (a) First cut from Figure 2, $\chi_{AD}N = -5$. Qualitatively similar to second cut at $\chi_{AD}N = 0$. (b) Third cut from Figure 2, along $\chi_{AD}N = 0.3$.

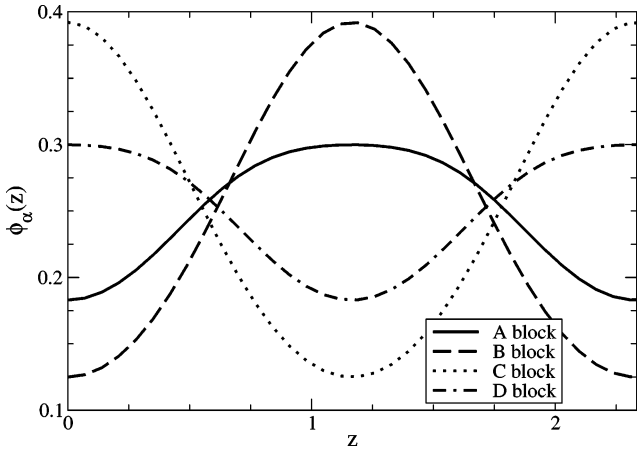

Figure 6. Monomer density profile for the mixed centrosymmetric AB lamellar phase (MCS AB) of the ABCD tetrablock copolymer melt with $f_\alpha = {}^1/_4$. The Flory−Huggins parameters are $\chi_{\alpha\beta}N = \chi N = 26$, $\chi_{BC}N = 43$, $\chi_{AD}N = -5.0$.

5a), with a slightly larger window in the phase space for the direct disorder-to-NCS transition (still centered around $\chi_{BC}N \simeq 42$). The presence of the NCS phase implies that the symmetric ABCA prefers interfaces between A1 and A2 rather than A1:A1 and A2:A2 interfaces (the number denotes block sequence (A1)BC-(A2)), indicating entropic effects which favor the NCS lamellar phase. The ABCA system will be investigated further in the next section. It is interesting to note that

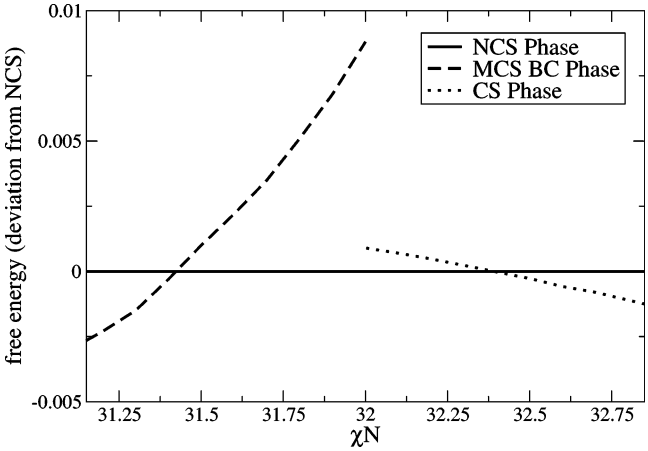

Figure 7. Free energy curves for each accessible lamellar phase for the ABCD tetrablock copolymer melt with $f_\alpha = {}^1/_4$. The Flory Huggins parameters are $\chi_{\alpha\beta} = \chi$ except $\chi_{AD}N = 0.3$. The free energies are shown relative to the NCS free energy.

the ABCA phase diagram does not show a CS phase, even at higher χN and higher $\chi_{BC}N$.

The phase diagram for the third cut in the $\chi_{BC}N - \chi N$ plane at $\chi_{AD}N = 0.3$ is shown in Figure 5b. A CS phase region is found for high χN, which slightly increases in size for larger $\chi_{BC}N$. The window for the direct disorder-to-NCS transition is slightly larger than for the previous two cuts, and is centered around $\chi_{BC}N \simeq 41.5$. The size of the NCS phase region increases with increasing $\chi_{BC}N$, but not to the degree shown in the previous two phase diagrams. As well, for values of $\chi_{BC}N < 29$, the NCS phase is not seen for any value of χN. It is interesting that below $\chi N \simeq 27$, the MCS BC to disorder to MCS AB behavior is identical for all three cuts. This indicates that these transitions are relatively independent of χ_{AD}.

The phase diagram shown in Figure 5b exhibits transitions between disorder to MCS BC to NCS to CS. The free energy differences between these phases near the transitions are shown in Figure 7. The small differences between the free energies require a high precision in computation. The transitions shown here are all first order, whereas there exists a second-order critical point in the ABC/ac blends.[1]

3.2. Entropic Effects. To investigate the entropic effects in the formation of the NCS lamellar phase, the compositions of the outer blocks in an ABCA tetrablock copolymer melt are varied. The effect of changing compositions on the phase behavior shown in Figures 2 and 5a is examined. Since unequal block compositions lead to nonzero interfacial curvature, the inner block compositions are kept equal ($f_B = f_C$) to maintain lamellar ordering. The outer blocks will be denoted by A1 and A2. To focus on the entropic effects, all enthalpic interaction parameters are set equal ($\chi_{AB} = \chi_{AC} = \chi_{BC} = \chi$).

As a first example, the relative volume fractions of all species are kept equal, $f_A = f_B = f_C = {}^1/_3$, where $f_A = f_{A1} + f_{A2}$. As f_{A1} is varied from 0 to ${}^1/_3$, the structure gradually converts from a BCA triblock with equal block compositions to an ABC triblock which is equivalent to the BCA triblock since all $\chi_{\alpha\beta}$ are equal. An ABCA tetrablock with shorter outer blocks compared to inner blocks is located at the center of the $f_{A1} - \chi N$ phase diagram.

The computed mean-field phase diagram is shown in Figure 8a. The phase diagram is symmetric about a

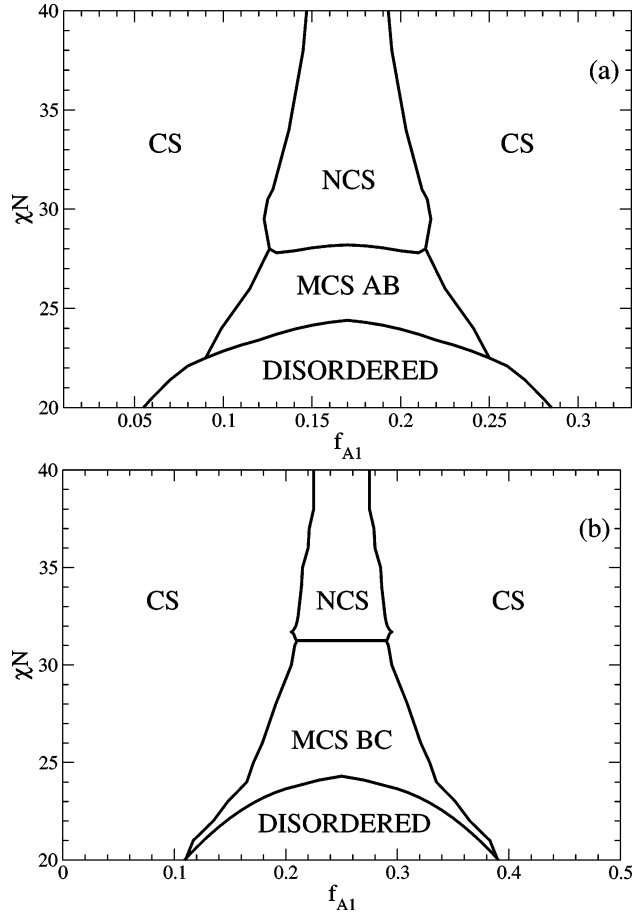

Figure 8. Mean-field phase diagram for the ABCA tetrablock copolymer melt with $\chi_{\alpha\beta} = \chi$ for (a) inner block compositions $f_B = f_C = 1/3$ (overall species volume fractions equal), and (b) inner block compositions $f_B = f_C = 1/4$.

midpoint of $f_{A1} = 1/6$. The $(\chi N)_{ODT}$ values decrease sharply from the tetrablock region (center) toward the triblock region, consistent with the earlier observation that higher χ values are required to induce ordering as the number of blocks increases. The regions where one of the outer blocks is very small show only CS phase behavior. This CS phase changes gradually from the region where the end A blocks have a significant and comparable size (to each other), where the sequence is ...ABCAACBA..., to the region f_{A1} or $f_{A2} \ll f_B$, where the small *A* block mixes with it's neighboring block. This produces the sequence ...ABCCBA... where f_{A2} is small and the analogous sequence when f_{A1} is small. The phase behavior in the central region is more complex. At the very center of the phase diagram, the disordered phase transforms into the MCS AB phase as χN increases. The NCS phase then becomes the equilibrium phase for $\chi N \geq 28$. Moving away from $f_{A1} = 1/6$, this MCS AB-to-NCS boundary continues until one of the outer blocks reaches a composition of roughly f_{A1} or $f_{A2} = 0.125$. At this point, the MCS AB phase converts into the CS phase, with a phase boundary that drops sharply. As well, the NCS region of phase space decreases in width as χN increases.

As a second example, we investigate the phase behavior for ABCA tetrablock copolymer melts with inner block lengths $f_B = f_C = 1/4$. As f_{A1} is varied from 0 to $1/2$, the polymer will change from a BCA triblock with the A block twice as long as the other two, to a similar ABC triblock. This makes it possible that the triblocks may form nonlamellar phases, but the tetrablock at the center of the phase diagram has equal compositions and likely forms an ordered lamellar structure.

The mean-field phase diagram for this system is shown in Figure 8b. As in Figure 8a, the phase diagram is symmetric about the midpoint, this time $f_{A1} = f_{A2} = 1/4 = f_B = f_C$, with $(\chi N)_{ODT}$ again decreasing sharply away from the central region. As well, the triblock region and the region where one of the outer blocks is much smaller than the other exhibit only CS phase behavior, as seen for larger inner blocks. There are also many differences in this phase diagram when compared to Figure 8a. First, while the order−disorder transition near the center seems to occur at nearly the same value of $(\chi N)_{ODT}$, the decrease is more rapid as the composition of the outer blocks changes. The system changes from a disordered phase to a mixed centrosymmetric phase, MCS BC in this case. The MCS BC phase persists to greater differences between f_{A1} and f_{A2} than for the first example, up to values of 0.11 for the smaller of the two outer blocks. The NCS phase is in equilibrium above $\chi N \simeq 31$, which results in a larger region occupied by the mixed centrosymmetric phase in this diagram. The NCS phase is narrower around the midpoint than in Figure 8a. A slight bulge is observed at the base of the NCS phase region ($\chi N \simeq 31$), similar to Figure 8a. The NCS region in phase space centers around $f_{A1} = f_{A2}$ for both cases, consistent with the arguments put forward by Amoskov and Birshtein,[14] as discussed in the next section.

It is interesting to note that different mixed phases are observed for the two cases shown in Figure 8. For the first case, $f_B = f_C = 1/3$, and the size of the outer blocks is $f_{A1} = f_{A2} = 1/6$ in the middle of the phase diagram. The outer blocks are much smaller than the inner blocks, and the observed phase above $(\chi N)_{ODT}$ is the MCS AB phase. As the repulsion between blocks increases and it becomes favorable to separate the blocks, block junction points are localized at an interface to form lamellar structures. This produces an entropic penalty to the free energy. For the ABCA polymer (with all $\chi_{\alpha\beta}$ equal), symmetry dictates that either the BC junction is localized at an interface, or the AB and CA junctions are both localized. In the former case, the resultant phase is the MCS AB phase. This phase is favorable if the A block is small enough that there is little enthalpic cost for mixing the A block with the B or C block. If the A block is larger, the enthalpic cost from this mixing is too high, and the system remains disordered until the enthalpic penalty leads to the localizing of both the AB and CA junctions. This situation is observed in Figure 8b, where $f_\alpha = 1/4$ in the middle of the phase diagram.

Neither of the phase diagrams in Figure 8 exhibit a direct disorder-to-NCS phase transition. The previous method to attain a direct transition involved breaking up the intervening mixed phase. The presence of two different mixed phases, one in each system, requires a different route. The difference between parts a and b of Figure 8 in the central region involves the length of the inner blocks. As $f_B = f_C$ is varied (with outer block compositions kept equal, $f_{A1} = f_{A2}$), if a disordered phase intervenes between the MCS AB and MCS BC phases, that would indicate the possibility of a direct disorder to NCS transition in that region. The phase diagram for this system in the $\chi N - f_B$ plane is shown in Figure 9.

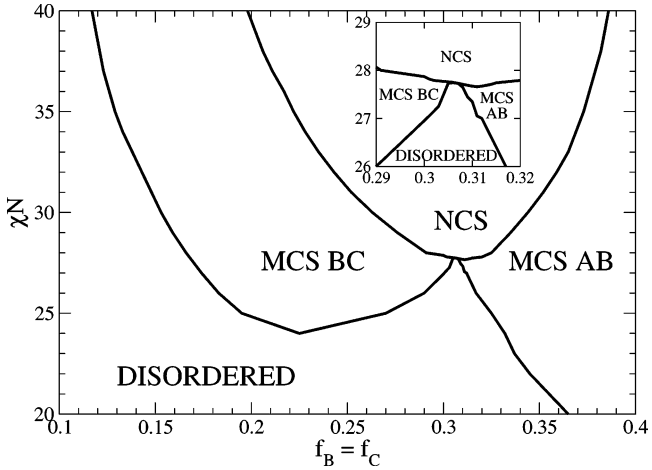

Figure 9. Mean-field phase diagram for the ABCA tetrablock copolymer melt with inner and outer blocks respectively symmetric ($f_{A1} = f_{A2}$, $f_B = f_C$), with $\chi_{\alpha\beta} = \chi$. The insert shows in greater detail the behavior near the direct disorder to NCS phase boundary.

For very low f_B and f_C, the tetrablock behaves like a homopolymer of A, resulting in a large region of the disordered phase. As f_B increases, the melt changes from the disordered phase to the MCS BC phase. The size of the MCS BC phase region in Figure 9 increases as f_B increases, to a maximum near $f_B = 0.2$ where $(\chi N)_{ODT}$ reaches a local minimum. Past this point, $(\chi N)_{ODT}$ increases while the χN value for the MCS BC−NCS transition decreases. This leads to a direct disorder-to-NCS transition in a small window of phase space near $f_B \simeq 0.306$. The MCS AB phase is observed for larger values of f_B and the MCS AB−NCS phase boundary increases rapidly. The χN for the disorder-to-MCS AB transition decreases quickly over this same range of f_B. The lower value of $(\chi N)_{ODT}$ is expected with the tetrablock becoming closer to a BC diblock. A direct disorder-to-NCS phase transition is obtained for an ABCA tetrablock copolymer with $f_B = f_C \simeq 0.306$, $f_{A1} = f_{A2} \simeq 0.194$.

4. Conclusions

The phase behavior of lamellar structures (Figure 1) in ABCD tetrablock copolymer melts has been examined using self-consistent mean-field theory. Both enthalpic and entropic effects were shown to yield a NCS lamellar phase. As well, through careful selection of parameters, direct disorder-to-NCS transition windows were found for several systems.

By varying the interaction between the first and fourth blocks ($\chi_{AD}N$) from slightly repulsive to slightly attractive (Figure 2), a NCS phase was stabilized and found to occupy a large region of the phase diagram where A and D are attractive. The NCS phase was also found in a small window of phase space for $\chi_{AD} > 0$. A partially mixed phase (MCS BC) is observed between the disordered and fully ordered CS and NCS phases. By varying $\chi_{BC}N$, the B and C blocks can be separated, destroying the MCS BC phase and yielding a disorder to NCS phase transition (Figure 5) in three separate cases: (a) $\chi_{AD}N = -5$, (b) $\chi_{AD}N = 0$ (the ABCA tetrablock copolymer), and (c) $\chi_{AD}N = 0.3$. All three systems also exhibit a new mixed phase, MCS AB (Figure 6), which is the equilibrium phase above χN_{ODT} at high $\chi_{BC}N$. The requirement to localize one junction

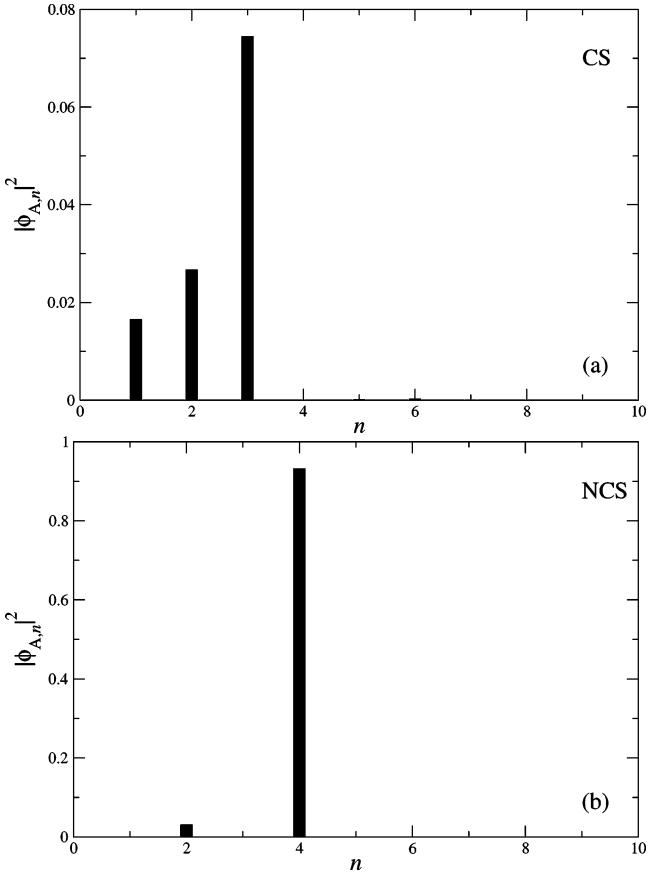

Figure 10. Histograms of $|\phi_{A,n}|^2 \equiv |\phi^{(c)}_{A,n}|^2 + |\phi^{(s)}_{A,n}|^2$ as a function of n, with $\chi N = 32$ and $\chi_{AD}N = 0.3$, for (a) metastable CS lamellar phase and (b) stable NCS lamellar phase. Note the change in scale for the y-axis. Coefficients with higher values of $n > 4$ are invisible at this scale.

(versus two for MCS BC) allows the window for this phase to extend to low χN.

Besides a difference in the periods, the structural difference between the CS and NCS phases could also be detected using scattering techniques. The intensities at the Bragg peaks would correspond to the square of the Fourier coefficients of the density profiles. The Fourier coefficients of CS and NCS phases are presented in Figures 10 and 11. Clear differences in the postions and amplitudes between these two structures are shown.

The entropic effects on stabilizing the NCS phase were investigated by varying the relative block compositions of the A-species in ABCA tetrablock copolymers. In the case where all species volume fractions are equal, as well as in the case where the inner blocks represent half the total polymer composition ($f_B = f_C = 0.25$), the NCS phase was found to be favored when the outer blocks were roughly equal in composition. The two systems do show a difference in the region between the disordered phase and the NCS phase. For larger f_B and f_C, a MCS AB phase is found, whereas a MCS BC mixed phase is observed for smaller f_B and f_C. By varying $f_B = f_C$ and keeping the two outer block compositions equal to each other, a direct disorder-to-NCS phase transition is found for a small region of phase space (Figure 9). No direct transition between the two mixed phases has been found.

Previous theoretical studies of entropically stabilized NCS phase depend on asymmetric interfaces[13] or asymmetric grafting densities.[14,15] The conclusion of ref 14

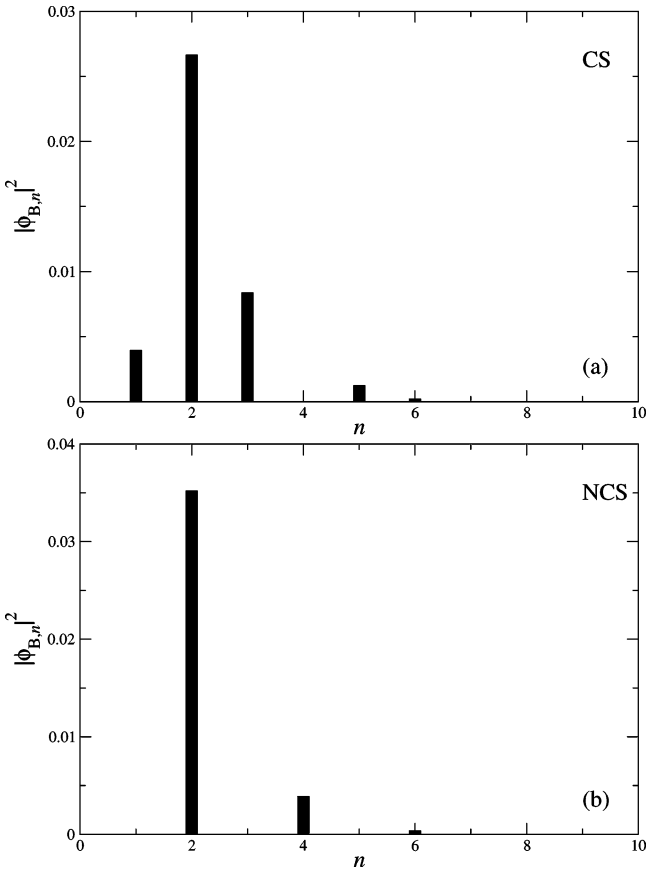

Figure 11. Histograms of $|\phi_{B,n}|^2 \equiv |\phi^{(c)}_{B,n}|^2 + |\phi^{(s)}_{B,n}|^2$ as a function of n, with $\chi N = 32$ and $\chi_{AD}N = 0.3$, for (a) metastable CS lamellar phase and (b) stable NCS lamellar phase. Note the change in scale for the y-axis.

indicates that both equal and unequal block lengths result in symmetric interfaces. However, the energetic contribution from these interfaces is favorable to formation of NCS structures for equal block lengths, and unfavorable for unequal block lengths. For the case of blends, the unequal block lengths are countered by the favorable contribution to the free energy from the asymmetric grafting densities. In this paper, SCMFT calculations have shown regions of NCS lamellar phase where the two outer blocks of the polymer are roughly equal in size. This result is consistent with our previous work,[1] and consistent with the results for equal block lengths.[14]

The results of this study indicate that both enthalpic and entropic effects can lead to a NCS lamellar phase, and can yield direct disorder-to-NCS phase transitions. Only lamellar structures have been considered in this study. Block compositions were chosen such that curved interfaces are not favored. This would indicate that further work will be needed to determine the global behavior of these lamellar phases in the full phase diagram for the ABCD tetrablock copolymer. This work has demonstrated that NCS phases can be formed in principle, within SCMFT, in these systems. Although the calculations presented in this paper were carried out for the cases with many of the interaction parameters set to equal, we expect that the general picture developed here for the mechanism of formation of NCS phases to be robust to small variations in the other $\chi_{\alpha\beta}$ away from equality.

Recently, Takano and co-workers have published experimental studies[18,19] on the lamellar behavior of tetrablock copolymers. A tetrablock ABCD melt was shown in ref 18 to exhibit centrosymmetric lamellar behavior for the case where the A and D blocks are almost compatible ($\chi_{AD} = 3.33 \times 10^{-3}$ at 418 K), while the other interaction parameters are not given and the volume fractions of all the blocks are unequal ($f_A = 0.25$, $f_B = 0.23$, $f_C = 0.32$, $f_D = 0.20$). On the basis of the phase diagram given in Figure 2, we predict that a careful annealing of the system from the disordered phase should yield a mixed centrosymmetric phase (MCS BC or MCS AB) before reaching the fully separated CS phase. In addition, given the low χ_{AD} it is possible that the system may exhibit NCS lamellar behavior similar to that seen in the lip region of Figure 2.

In ref 19, Takano and co-workers demonstrated that an ABCA tetrablock copolymer melt exhibits a noncentrosymmetric lamellar structure for $f_{A1} = f_{A2} = 0.23$, and $f_B = 0.24$, $f_C = 0.30$. While the effects of unequal B and C block volume fractions and unequal interaction parameters are unknown, the observation of a NCS lamellar phase for equal A1 and A2 block lengths is consistent with the theoretical work in this paper. The inset shown in Figure 9 details the order−disorder-transition behavior for an ABCA melt with equal B and C block lengths. According to this phase diagram, we predict that, if the system in ref 19 is carefully annealed, there are two possibilities. From the disordered phase, the system will either pass through a mixed CS phase (MCS BC or MCS AB) or directly into the NCS lamellar phase. It will be very interesting if this theoretical prediction can be tested by such an experiment.

Acknowledgment. The authors would like to thank Prof. Edwin L. Thomas for very helpful discussions, SHARCNET for computing resources, and Mr. David Cooke for his aid in optimizing the numerical procedure. This work was supported by the Natural Sciences and Engineering Research Council of Canada (NSERC), the Research Corporation, and Ontario Premier's Research Excellence Award.

References and Notes

(1) Wickham, R. A.; Shi, A.-C. *Macromolecules* **2001**, *34*, 6487−6494.
(2) Tournilhac, F.; Blinov, L. M.; Simon, J.; Yablonsky, S. V. *Nature (London)* **1992**, *359*, 621−623.
(3) Stupp, S. I.; LeBonheur, V.; Walker, K.; Li, L. S.; Huggins, K. E.; Keser, M.; Amstutz, A. *Science* **1997**, *276*, 384−389.
(4) Petschek, R. G.; Wiefling, K. M. *Phys. Rev. Lett.* **1987**, *59*, 343−346.
(5) Halperin, A. *Macromolecules* **1990**, *23*, 2724−2731.
(6) Goldacker, T.; Abetz, V.; Stadler, R.; Erukhimovich, I.; Leibler, L. *Nature* **1999**, *398*, 137−139. Goldacker, T.; Abetz, V.; Stadler, R. *Macromol. Symp.* **2000**, *149*, 93−98.
(7) Hamley, I. W. *The Physics of Block Copolymers*; Oxford University Press: Oxford, England, 1998.
(8) Hadjichristidis, N.; Pispas, S.; Floudas, G. *Block Copolymers: Synthetic Strategies, Physical Properties, and Applications*; Wiley-Interscience: New York, 2003.
(9) Matsen, M. W.; Schick, M. *Phys. Rev. Lett.* **1994**, *72*, 2660−2663.
(10) Zheng, W.; Wang, Z.-G. *Macromolecules* **1995**, *28*, 7215−7223.
(11) Abetz, V.; Goldacker, T. *Macromol. Rapid Commun.* **2000**, *21*, 16−34.
(12) One exception is the helical structure, discussed in: Krappe, U.; Stadler, R.; Voigt-Martin, I. *Macromolecules* **1995**, *28*, 4558−4561.
(13) Leibler, L.; Gay, C.; Erukhimovich, I. *Europhys. Lett.* **1999**, *46*, 549−554.
(14) Amoskov, V. M.; Birshtein, T. M. *Polym. Sci., Ser. A.* **2002**, *44*, 959−974.

(15) Birshtein, T. M.; Polotsky, A. A.; Amoskov, V. M. *Macromol. Symp.* **1999**, *146*, 215−222. Amoskov, V. M.; Birshtein, T. M.; Pryamitsyn, V. A. *Macromolecules* **1998**, *31*, 3720−3730.
(16) Doxastakis, M.; Chrissopoulou, K.; Aouadi, A.; Frick, B.; Lodge, T. P.; Fytas, G. *J. Chem. Phys.* **2002**, *116*, 4707−4714. Takahashi, K.; Hasegawa, H.; Hashimoto, T.; Bellas, V.; Iatrou, H.; Hadjichristidis, N. *Macromolecules* **2002**, *35*, 4859−4861. Chrissopoulou, K.; Tselikas, Y.; Anastasiadis, S. H.; Fytas, G.; Semenov, A. N.; Fleischer, G.; Hadjichristidis, N.; Thomas, E. L. *Macromolecules* **1999**, *32*, 5115−5126. Chapman, B. R.; Hamersky, M. W.; Milhaupt, J. M.; Kostelecky, C.; Lodge, T. P. *Macromolecules* **1998**, *31*, 4562−4573.
(17) Drolet, F.; Fredrickson, G. H. *Phys. Rev. Lett.* **1999**, *83*, 4317−4320. Drolet, F.; Fredrickson, G. H. *Macromolecules* **2001**, *34*, 5317−5324.
(18) Takano, A.; Soga, K.; Asari, T.; Suzuki, J.; Arai, S.; Saka, H.; Matsushita, Y. *Macromolecules* **2003**, *36*, 8216−8218.
(19) Takano, A.; Soga, K.; Asari, T.; Suzuki, J.; Matsushita, Y. *Macromolecules* **2003**, *36*, 9288−9291.
(20) Lee, J. H.; Balsara, N. P.; Chakraborty, A. K.; Krishnamoorti, R.; Hammouda, B. *Macromolecules* **2002**, *35*, 7748−7757. Reichart, G. C.; Graessley, W. W.; Register, R. A.; Krishnamoorti, R.; Lohse, D. J. *Macromolecules* **1997**, *30*, 3036−3041.
(21) Helfand, E. *J. Chem. Phys.* **1975**, *62*, 999−1005. Hong, K. M.; Noolandi, J. *Macromolecules* **1981**, *14*, 727−736.
(22) Shi, A.-C.; Noolandi, J.; Desai, R. C. *Macromolecules* **1996**, *29*, 6487−6504.
(23) Shi, A.-C. In *Developments in Block Copolymer Science and Technology*; Hamley, I. W., Ed.; Wiley & Sons: New York, 2004; p 265.
(24) There is no evidence of a mixed phase where A and C mix together and the B and D blocks mix together (Figure 1e) due to the entropic barrier to such a phase (all three tetrablock junctions would be localized at interfaces).

MA049784H